Multi-stations sheet metal assembly modeling and diagnostics

B.W. Shiu, D. Ceglarek
Department of Mechanical Engineering and Applied Mechanics
University of Michigan
Ann Arbor, MI

J. Shi
Department of Industrial and Operations Engineering
University of Michigan
Ann Arbor, MI

ABSTRACT.

In this paper, a multi-station assembly process is modeled for diagnosing automotive body dimensional faults. The proposed approach enables multi-station assembly process modeling based on design information (CAD) and allows system behavior determination based on the in-line measurements of the final product. The method includes generic modeling of the key assembly process characteristics; tooling types and locations, as well as part-to-part joints. The modeling is based on the pre-determined variation patterns caused by failures of each selected characteristic. The proposed model successfully diagnosed multiple dimensional faults of an automotive body assembly process. Verification of the proposed method is presented through an actual case study.

INTRODUCTION

Increasing quality and productivity are two major goals in today's automotive industry. Fixture failure and dimensional variation is one of the major factors to decrease productivity (manual adjustments on doors, fenders and hoods) as well as quality (water leaks, closing effort and wind noise). Currently, automotive assembly plants rely on trial and error to locate sources of variation and system faults, which requires years of experience and knowledge of the assembly process/product design. Traditionally, SPC (Statistical Process Control) (Faltin & Tucker, 1991) is the standard method for controlling the process and maintaining a high dimensional quality of product. With the recent introduction of OCMM (Optical Coordinate Measurement Machine), and the availability of 100% measurements, advanced quality control techniques are required to take advantage of this information (Hu & Wu, 1990, Roan et al., 1993, Ceglarek et al., 1994). A diagnostic technique based not on heuristic information but on the first principle, system model, is necessary for today's requirement of fast model change over (Davis, 1983, Reiter, 1987). Currently, in the area of sheet metal assembly, a method developed to model fixture failures proves the identical relationship between the Principle Component Analysis (PCA) and the fixture tooling failures (Ceglarek & Shi, 1996). However, this method only focused on the single assembly fixture failure.

This paper focuses on the development of a multi-station assembly modeling methodology for diagnostics of the automotive body assembly process. In this paper, a multi-station assembly process is modeled based on critical characteristics of the assembly process, such as the locating mechanism which controls the orientation and location of parts and the part-to-part mating geometry which describes the joining conditions. A diagnostic reasoning strategy is developed by matching model behavior to the real behavior of an automotive body assembly process that obtained through in-line 100% measurements.

In this paper, automotive body assembly process will be introduced first. Then, modeling based on the critical feature of the single assembly station is described and followed by the modeling of multi-stations process. Next, the fault propagation model is introduced. Finally, simulation results of single and multiple faults diagnostics and a case study based on the real industrial data are presented.

AUTOMOTIVE SHEET METAL ASSEMBLY

This section describes the automotive body structure and assembly process design. Automotive body manufacturing is a complicated sheet metal assembly process because of the complex body structure. A typical automotive body is made of 200-250 sheet

metal parts assembled in 60 -100 assembly stations with 1700 to 2100 different types of locators. The Body-In-White (BIW), as shown in Figure 1, can be defined as an automotive body without closure panels such as: doors, hood, fenders, and deck lid, and without powertrain and chassis accessories. A BIW is the basic structure of the whole vehicle. In general, a BIW is made from three major subassemblies such as the underbody, the left and right hand side frames, and the roof. Each major subassembly is made of smaller subassemblies or parts.

FIGURE 1. Body-In-White (BIW)

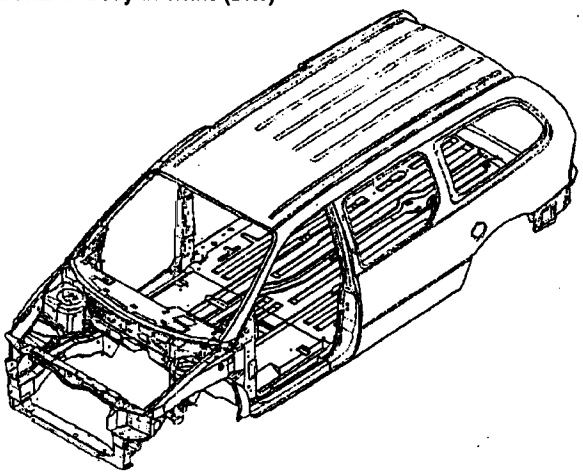

The main factors of the assembly process having impact on the BIW dimensional integrity are: (1) locating mechanisms in geometrical assembly stations, and (2) part-to-part interaction.

Locating mechanism in assembly process design

Geometrical assembly stations are designed to assemble two or more parts together. They consist of locating mechanisms, joining equipment, and parts transferring mechanisms. Due to the functionality of a geometrical assembly stations, the most important source of dimensional non-conformance would be contributed by the failure of locators within such assembly stations. Locators and their locating schemes for part positioning consist of one basic building block called "3-2-1" or "n-2-1" schemes designed for rigid parts, and flexible parts respectively. The fixture and locators' function are to position the parts in space correctly. Theoretically, a 3-2-1 locator scheme as shown in Figure 2 would be sufficient to orient and locate a rigid part in space.

FIGURE 2. A typical 3-2-1 scheme for rigid sheet metal

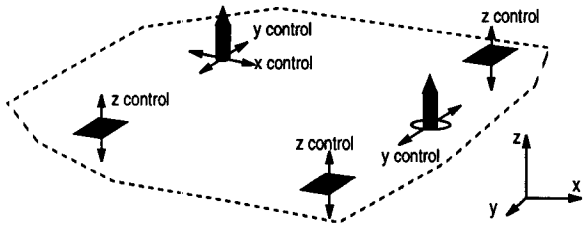

The 3-2-1 locating method utilizes fundamental geometry. Three points in space generate a plane, two points in addition to this first plane would generate a second plane perpendicular to it, while one final point generates a third plane perpendicular to the other two. Therefore, an xyz coordinate system would be generated in space to locate and orient a part. This locating method is the backbone of the simulation process where part location is determined by the locator description or design. In addition, the locating scheme depends on the method of joining and their part-to-part interaction, which will be discussed in the next section.

On today's manufacturing floor, locators, as shown in Figure 3, are divided into three different categories: (1) 2-way or 4-way locating pins; (2) NC locating block with part holding clamp; and (3) the NC locating blocks without clamp. A 4-way locating pin gives four direction control. Locating pins are used extensively because the position of locating holes can be stamped very consistently in relation to the part's geometry. An NC block with clamp gives a two direction control while NC block gives one direction control.

FIGURE 3. Types of locators

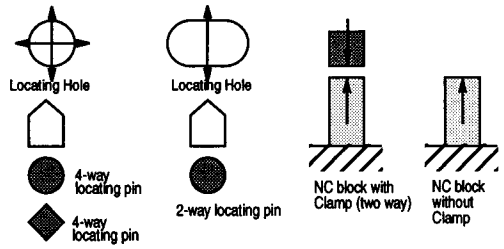

Part-to-part interaction

One of the most critical elements in BIW design is part-to-part interaction. Part-to-part interactions stern from the characteristics of the joining interface. These interactions can be characterized into three main types of joints (Ceglarek & Shi, 1995) in an automotive body as shown in Figure 4: (1) lap-to-lap joints (two flat sheet metal pieces overlap to form a joint), (2) butt-to-butt joints (two flanged parts joined at their flanges), and (3) lap-to-butt joint (one flanged piece and one flat piece joined together at their edges).

Each type of joints exhibits a different characteristic and behavior. Lap-to-lap joints tend to allow slip plane movement along the plane of the sheet metal. Butt-to-butt joints tend to constrain the movement in the sheet metal plane. Lap-to-butt exhibits a combination of both characteristics. Behavior resulting from these part-to-part interactions will be discussed and modeled in the next section.

FIGURE 4. Three main types of joints

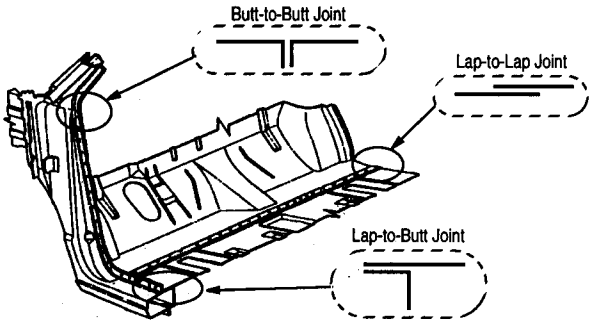

GENERIC MODELING OF SINGLE STATION

In general, as mentioned in the previous section, there are three typical joints in the sheet metal assembly: (1) a lap-to-lap joint, (2) a butt-to-butt joint, (3) a lap-to-butt joint. This section presents modeling of lap-to-lap joint. The modeling of butt-to-butt and

lap-to-butt joints are presented in Shiu (1995). Figure 5 shows the top view of the lap-to-lap joint. T^a1, T^a2, to T^am represents the tooling geometry of part *a* at points from 1 to m respectively. P^a1, P^a2, to P^an represents the part *a* geometry at various geometrical points from 1 to n respectively, similarly for part *b* where superscripts are replaced by superscript b.

FIGURE 5. Lap-to-Lap joints

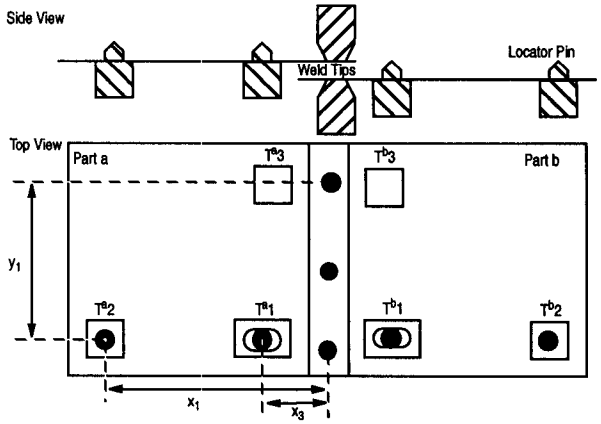

Part *a* and *b* are located based on a 3-2-1 scheme. The z direction is set by joints (welds), position of fixture locators and parts geometry. The lap-to-lap joints are not constrained by part interference in x-y plane. Thus, lap-to-lap joint can be characterized as rotations and translations in x-y plane. The side view indicates the weld tips accessing the parts from the top.

TABLE 1. Categories of dimensional faults caused by the locators

Fault One T^a1	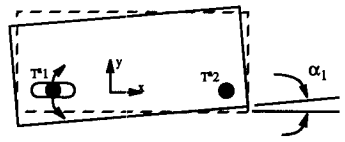 Part Movement
Eq. 1	$\begin{bmatrix} P^a1_x \\ P^a1_y \\ P^a1_z \end{bmatrix}_{i+1} = \begin{bmatrix} \cos\alpha_1 & \sin\alpha_1 & 0 \\ -\sin\alpha_1 & \cos\alpha_1 & 0 \\ 0 & 0 & 1 \end{bmatrix} \begin{bmatrix} P^a1_x - T^a2_x \\ P^a1_y - T^a2_y \\ P^a1_z - T^a2_z \end{bmatrix}_i + \begin{bmatrix} T^a2_x \\ T^a2_y \\ T^a2_z \end{bmatrix}$
Fault Two T^a2	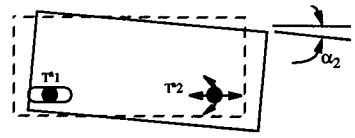 Part Movement
Eq. 2	$\begin{bmatrix} P^a1_x \\ P^a1_y \\ P^a1_z \end{bmatrix}_{i+1} = \begin{bmatrix} \cos\alpha_2 & \sin\alpha_2 & 0 \\ -\sin\alpha_2 & \cos\alpha_2 & 0 \\ 0 & 0 & 1 \end{bmatrix} \begin{bmatrix} P^a1_x - T^a1_x \\ P^a1_y - T^a1_y \\ P^a1_z - T^a1_z \end{bmatrix}_i + \begin{bmatrix} T^a1_x \\ T^a1_y \\ T^a1_y \end{bmatrix} + \begin{bmatrix} T^a2_x \\ 0 \\ 0 \end{bmatrix}$
Multiple faults T^a1 & T^a2	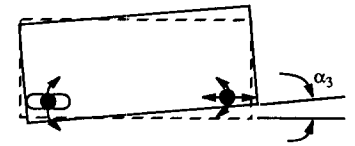 Part Movement
	Combination of above two equations

Table 1 shows different locator failures patterns for a lap-to-lap joint. If T^a1 is at fault, the x direction would not affect the final dimension because of the characteristics of a two way locating pin. On the other hand, the y direction would affect final dimension. Part *a* will be pivoted about T^a2 locator. The rotation angle caused by T^a1 in y direction is denoted by $\alpha_1 = \text{atan}\left(\frac{T^a1_y}{x_1 - x_3}\right)$. Equation 1 demonstrates the effect of T^a1 in y direction variation. The failure of T^a2 locator provides both x and y direction errors. A rotation of part *a* about T^a1 can be observed by the y direction movement of locating pin T^a2. The x direction translation of T^a2 would result in whole part *a* movement in the x direction. Equation 2 demonstrates the effect with rotation angle $\alpha_2 = \text{atan}\left(\frac{T^a2_y}{x_3 - x_1}\right)$. Multiple faults created by T^a1 and T^a2 demonstrate a combination of part *a* movement that resulted from both equations. The total effect of these faults can be calculated in a sequential computation where one transformation is performed after the other.

GENERIC MODELING OF MULTIPLE STATIONS

Once two parts are assembled, the subassembly will be transferred to the next station. The parts are positioned according to consecutive station's locating scheme. Therefore, the subassembly is "re-oriented" according to the next station's tooling layout. For example, Figure 6 shows the assembly of rear quarter panel and fender beam to the aperture in the k station. Next operation of assembly process will be performed in the k+1 station.

Since a different set of locators are used in the k and k+1 station, any incorrect positioning of the aperture relative to the outer body panel in the k station would results in an observed fault at the k+1 station as shown with the dashed lines in Figure 6. Therefore, errors in station k would stack up to future assembly processes.

FIGURE 6. An example of the re-orientation concept

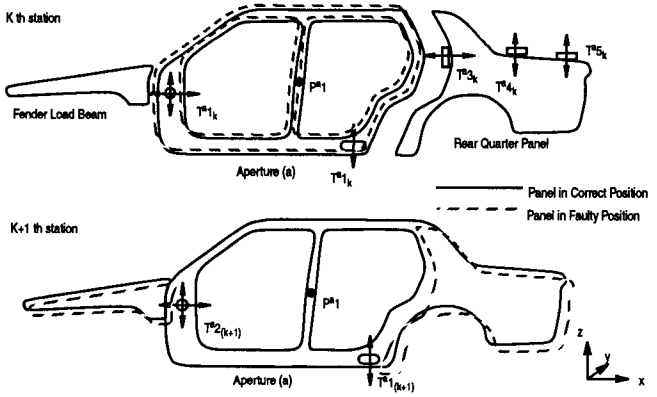

The Re-orientation transformation

The re-orientation is defined as repositioning due to transferring parts between stations that consist of different locating method. The re-orientation model is shown in the following equation for three planes, xy, xz, yz, rotation which represented angle α, β, γ and translation transformation.

$$\begin{bmatrix} {}^{a}P1_x \\ {}^{a}P1_y \\ {}^{a}P1_z \end{bmatrix} = \begin{bmatrix} \cos\alpha & \sin\alpha & 0 \\ -\sin\alpha & \cos\alpha & 0 \\ 0 & 0 & 1 \end{bmatrix} \begin{bmatrix} 1 & 0 & 0 \\ 0 & \cos\beta & \sin\beta \\ 0 & -\sin\beta & \cos\beta \end{bmatrix} \begin{bmatrix} \cos\gamma & 0 & \sin\gamma \\ 0 & 1 & 0 \\ -\sin\gamma & 0 & \cos\gamma \end{bmatrix} \begin{bmatrix} {}^{a}P1_x - {}^{a}T2_x \\ {}^{a}P1_y - {}^{a}T2_y \\ {}^{a}P1_z - {}^{a}T2_z \end{bmatrix} + \begin{bmatrix} {}^{a}T2_x \\ {}^{a}T2_y \\ {}^{a}T2_z \end{bmatrix}$$

${}^{a}T2_{(k+1)}$ is an illustrative datum location in 3 coordinates at the re-orientation station k+1, (Figure 6). ${}^{a}P1$ is being an example point located anywhere in the aperture.Those three points are also a rotation datum for the re-orientation geometry. The angle α,β,γ are obtained by the tooling differences in x,y,z direction respectively.

For example, $\alpha = \frac{({}^{a}T2_x)_{i+1} - ({}^{a}T2_x)_i}{l}$ is calculated from the difference of x direction tooling location between the k th and k+1 th station and anchor distance *l* (Figure 6).

Example of 3-Part 2-Station Assembly Process

The section shows the methodology of using the three parts assembly in two stations and the re-orientation concept. This three parts assembly consists of part *a, b, c* shown in Figure 7. In the assembly, joints between parts *c* and *a*, between parts *a* and *b*, and between parts *b* and *c* are lap-to-butt joint. These three parts are assembled in stations one and two (Figure 7).

FIGURE 7. Three Parts Assembly

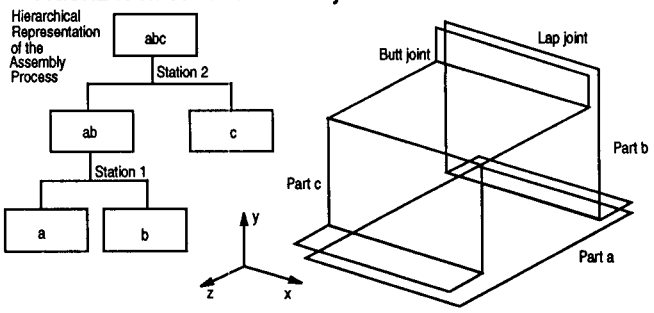

The station one

Figure 8 shows the two parts assembly in the first station. The geometric governing equations are the same as those of the lap-to-butt joint (Shiu, 1995).

FIGURE 8. The first station

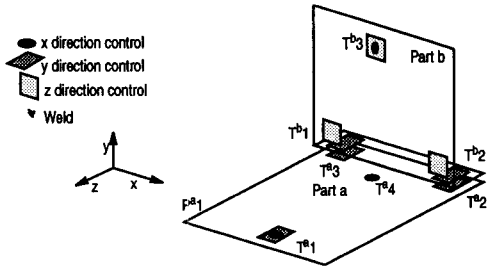

Station two and the Re-orientation

As shown in Figure 8 and Figure 9, station 1 and 2 have the same 3-2-1 locating scheme, but positions of locators between both stations are different. As noted in an earlier section, the re-orientation matrix applies to parts that are transferred from one station to the next. Therefore, a welded part is "re-oriented" according to the next station's tooling layout. The assembled part is designed to have a 3-2-1 scheme. Locators $T^{c}1$, $T^{c}2$, and $T^{c}3$ locators are used for controlling y direction. $T^{c}4$, and $T^{c}5$ control z direction. Additionally, the $T^{c}3$ locator is a two-way pin that controls the x direction. There are two modes of re-orientation rotation in this particular case. The first mode of re-orientation is caused by $T^{c}1$ and $T^{c}2$ resulting in a rotation about the z axis. The second mode of re-orientation is caused by $T^{c}3$ in relation to $T^{c}1$ and $T^{c}2$. Equation 1 shows the effect of first mode re-orientation:

FIGURE 9. The station two and its locating scheme

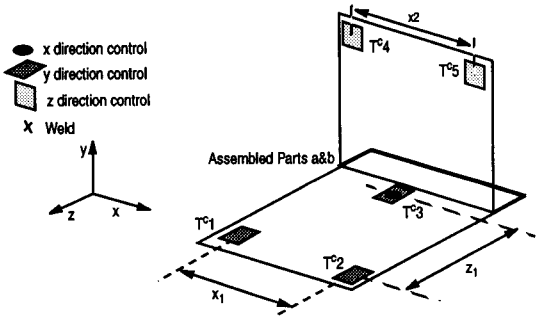

Station two assembly

Figure 10 shows the locating layout of part c. If either the $T^{c}1$ or $T^{c}7$ locator has problem, a rotation about the x axis will occur, because the three y direction locators ($T^{c}1$, $T^{c}2$, $T^{c}7$) would generate a plane that rotates about the x axis. Locator $T^{c}7$ is a two way pin that controls the y direction.

FIGURE 10. Next Station Assembly

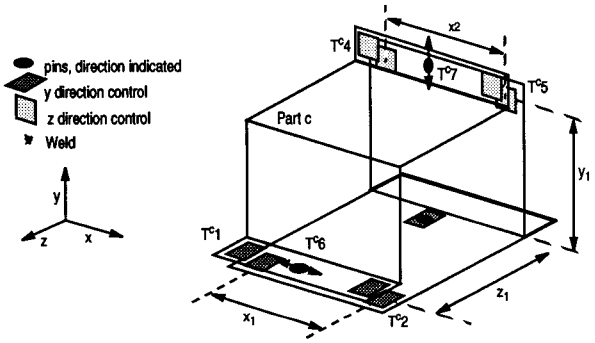

SIMULATION OF SINGLE/MULTIPLE FAULT(S)

A single and multiple fault(s) have distinctive variation patterns. The representation of a variation pattern can be expressed by a correlation matrix. As a result, correlation matrix changes can indicate the change in variation pattern. Multiple faults cause a more complicated pattern than that of the single fault. Variation patterns are generated by simulating the variations of locators positions. A single locator fault is simulated by the variation of a locator position for a given variance and mean. Similarly, a multiple locator fault is simulated by varying multiple locator locations with certain variance and mean.

An example of Lap-to-Lap joint fault patterns

The following describes an example of lap-to-lap joint diagnosis with single and multiple faults. Part movement is simulated by a

randomly generated locator position. Re-orientation follows after the assembly. As indicated in Table 1, there are a total of 7 possible combination of faults among T^a1 and T^a2 that would exist in this simulation. The program uses the governing equations (1) and (2) in Table 1, with locating scheme illustrated in Figure 5.

Simulation of one fault

Single fault of locator T^a1 for a given arbitrary magnitude is simulated for tooling layout shown in Table 1. The variation of tooling locator T^a1 cause variation of part *a*, which detected by measurement points P^a1 through P^a6. The variation of part *a* movement can be calculated based on Equation 1 for a given variation of the position of locators. Correlation can be generated based on these simulated parts position. The correlation matrix for a given correlation threshold (0.65) is presented in graphical form as a correlation map in Figure 11. Thus, the pattern shown in Figure 11 represents a correlation exceeding threshold 0.65. The right side of Figure 11 shows an empty negative correlation matrix, which indicates that there are no negatively correlated point in parts *a* and *b*. The left side of Figure 11 shows three groups of correlated points: (1) group one: P^a1, P^a2, P^a3; (2) group two: P^a4, P^a5, P^a6; (3) group three: all points in part *b*. Part *b* is being moved in x direction because the x direction datum is set at the T^a1. Therefore, part *b* is positively correlated in the x direction only by the re-orientation datum.

The simulated points are located around the part, P^a1, P^a2, P^a3 are located on the left side of part *a*, whereas, P^a4, P^a5, P^a6 are located on the right side of part *a*. Likewise, P^b1 to P^b3, and P^b4 to P^b6 are located on the left and right side of part *b* respectively.

FIGURE 11. One fault, left is positive, right is negative correlation

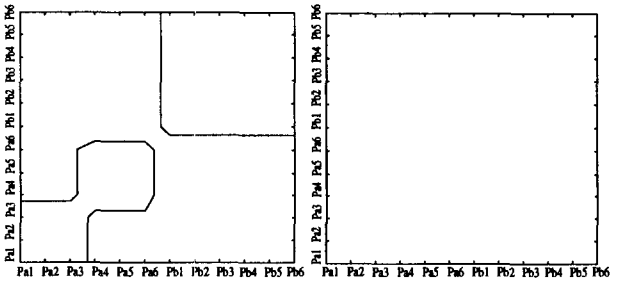

Simulation of the three faults

Figure 12 shows the contour map of the correlation matrix after the simulation of the three faults which include the faults of locators: T^a1 x and y direction, and T^a2 y direction. The complexity of the patterns increases when multiplicity of faults increases (Figure 11, and 12).

Three and one groups of positively and negatively correlated points can be found respectively (Figure 12):

(1) group one: P^a1, P^a4;

(2) group two: P^a2, P^a3, P^a5, P^a6;

(3) group three: from P^b1 to P^b6.

(4) negatively correlated group; P^a4 to P^a2, P^a3, P^a5, and P^a6.

From these correlation groups, one can conclude that the top and bottom portion of the part is swinging in opposite direction about a center close to the lower part of part *a*. Therefore, it can be concluded that there are two root causes. The first root cause is indicated by groups one, two, and four. The top part of part *a* is swinging in an opposite direction to the bottom part *a*. This movement can be generated by T^a1 and T^a2's y direction control because rotation about either one of the locators would result in negative correlation between the top and bottom of the part. Thus, we conclude that either T^a1 or T^a2's y direction control is experiencing a variation. The second root cause is indicated by group three. Part *b* is moving together in one direction. This indicates that part *a* is moving in the x direction. When part *a* is assembled into part *b*, part *b* behaves as if it were moving in the x direction.

FIGURE 12. Three faults, positive and negative correlation

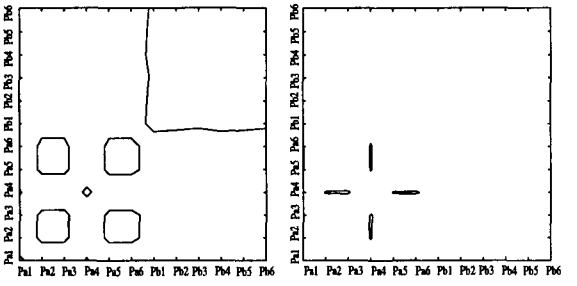

IMPLEMENTATION AND EVALUATION

The presented methodology was validated in a domestic automotive assembly plant. A case study related to a failure of 2-way locator during wheel house subassembly is presented in this section. Figure 13 shows wheel house and floor assembly with marked tooling locations. The wheel house is a Lap-to-Butt joint to the underbody.

FIGURE 13. Schematic of the assembly operation

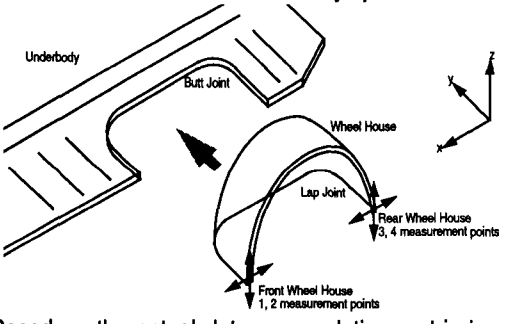

Based on the actual data, a correlation matrix is calculated and a correlation map is generated by showing the points bigger than 0.65. Figure 14 indicates a single correlated group with points 1 and 2 which are positioned at the front locating hole on the wheel house. Having extracted the faulty data from the front wheel house data, the correlation matrix is calculated. The observed correlation map is shown below with the threshold set at 0.65, which is based on the practical experience observed in the manufacturing floor.

FIGURE 14. Observed Correlation Map

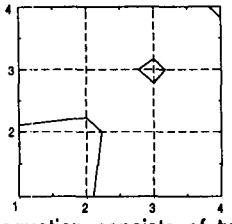

The simulation equation consists of two major transformations. First transformation is the rotation caused by the misgaged front pin. Rotation about the rear pin can be observed.The model-based Correlation Matrix shows a very similar result. In Figure 15, three different types of faults are simulated. Fault one indicates the front locating hole misgaging error. Fault two indicates rear locating hole misgaging error. Fault one and two indicates both locating hole misgaging error. Only fault one matches the observed data.

FIGURE 15. The Simulated Correlation Map

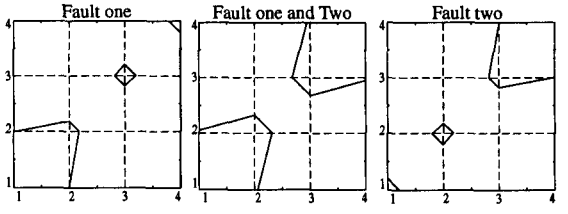

After verifying the assembly process, the problem was caused by misgaging the pin to the part. This case study indicates the applicability of the modeling to the diagnostic. An accurate model is required for the use of the diagnostic tools developed. The accuracy depends on the ability to simulates the real event verse the computational savings of the simplified model. A model which considers locators and joint characteristics is fundamentally necessary and important to the success of the diagnostic model. This case study verifies the comprehensiveness of modeling, including locators and part-to-part interaction.

SUMMARY AND CONCLUSION

The dimensional quality and integrity of sheet metal assemblies is one of the most important factors in autobody assembly. Hence, part positioning and part-to-part joining are critical elements in sheet metal assembly system. The correct and comprehensive modeling of those critical elements is very important in identifying and locating any dimensional malfunction of the systems. This paper develops comprehensive modeling principles for single as well as multiple assembly stations.

The single station modeling is based on part-to-part joint geometry classification and the 3-2-1 single part positioning layout. The joint geometry is classified into three types: lap-to-lap, butt-to-butt, and lap-to-butt joints. Each joint is modeled using the product/process design information.

The multi-station assembly system modeling extends the single station model by introducing the part re-orientation concepts. This concept identifies the relationship between two assembly stations by considering the impact of error accumulation from one station to the next. The developed model allows establishment of fault patterns for a combination of different part positioning schemes as well as part-to-part joint geometries. Even simultaneously occurring multiple faults can be diagnosed.

A case study based on real manufacturing process is presented. The results of the case studies demonstrate the effectiveness of the developed diagnostic approach.

REFERENCE

Ceglarek, D., Shi, J., 1995 "Design Evaluation of Sheet Metal Joints for Dimensional Integrity", *Proc. of the 1995 ASME International Mechanical Engineering Congress & Exposition,* MED vol. 1/DE vol. 86, pp. 117-128, San Francisco, CA.

Ceglarek, D., Shi, J., 1996 "Fixture Failure Diagnosis for the Autobody Assembly Using Pattern Recognition", *Trans. of ASME, Journal of Engineering for Industry,* vol. 118, no. 1.

Ceglarek, D., Shi, J., Wu S.M., 1994 "A Knowledge based Diagnosis Approach for the Launch of the Auto-body Assembly Process", *Trans. of ASME, Journal of Engineering or Industry* vol. 116, no. 4, pp. 491-499.

Davis, R., 1983 "Reasoning from First Principles in Electronic Troubleshooting." *Int. J. Man-Machine Studies*, 19, pp. 403-423.

Faltin, F.W., Tucker W.T., 1991 "On Line Quality Control for Factory of the 1990s and beyond," *Statistical Process Control in Manufacturing*, Keats J.B., Montgomery, D.C., Mercel Dekker Inc., 1991,

Hu, S.J., Wu S.M., 1990 "In-Process 100% Measurement and Statistical Analysis for an Automotive Body Assembly Process," *Trans. of NAMRI* vol. XVII, Penn. State University.

Reiter, R., 1987 "A Theory of Diagnosis from First Principles", *Artificial Intelligence* 32, pp. 57- 95.

Roan, C., Hu, S.J., Wu, S.M., 1993 "Computer Aided identification of Root Causes of Variation in Automotive Body Assembly", *Proceedings of the ASME Winter Annual Meeting*, PED vol. 64, pp. 391-400, New Orleans.

Shiu, B.W., 1995, "Feature Based Modeling of Automotive Assembly System for Diagnostics," Ph.D. Preliminary Examination, The University of Michigan, Ann Arbor.